Stiffened Sheathings of Orthotropic Cylindrical Shells

By P. Rigo[1]

Abstract: Geometric characteristics of orthotropic shells introduce computational difficulties (discretization of the stiffeners, computing time, interaction at the ring and stringer junctions with the sheathing, etc.). Navigation-dam gates, tidal surge barriers, etc., are hydraulic steel structures composed of orthotropic sheathings, which can now be more easily computed with the development of the LBR-3 stiffened sheathing software. This method is one of harmonic analysis and is founded on the Fourier series expansions. It is based on the analytical solution of the governing differential equations for orthotropic cylindrical shells. These differential equations result from the DKJ method (Donnell, von Kármán, and Jenkins) and allow taking into account the torsional stiffness, the lateral bending stiffness, and the exact position of each stiffener. New developments that permit the designing of stiffened cylindrical structures with many boundary conditions are presented. After the numerical verifications, an example of a tidal surge barrier design is presented.

Introduction

The requirements of longer spans, lighter structures, higher accuracy, etc., imposed on steel structures, have deeply changed their conception and design techniques. Nevertheless, it is disturbing to see that most of the hydraulic orthotropic structures (lock gate, movable weirs) are still computed as they were 30 years ago. The general bending of the structure is computed using any conventional method, and the results are added to those coming from the local stiffeners bending and to those resulting from local unstiffened shell deformation given by Timoshenko (1951), for example. In the last decade, digital simulation and finite-element method (FEM) improvements such as the superelement technique and computer-aided design (CAD) did not change this behavior much. One explanation could be that with FEM commercial software, there is a conflict between cost and accuracy. It is always possible to discretize a system smaller and smaller, but the computer storage capacity, the time one needs to discretize the system, and the budget may become limiting factors. Keeping these limitations in mind, the author would like to propose a new computerized method that can be economically used to design cylindrical orthotropic steel structures.

Rapid and accurate verification of the stresses and displacements at every point of a structure is the aim of this study. In spite of different stiffening schemes (ring, stringer, crossbar, as shown in Fig. 1), a computing tool (LBR-3) has been established without making simplications and approximations about structural geometry. Calculations are not based on smeared-out rib properties; rather, the torsional stiffness, the lateral (tangent to the shell) bending stiffness, and the exact position of each stiffener are taken into account. The stiffened sheathing method (SSM), the source of the LBR-

[1]Res. Assoc., FNRS, Naval Arch. Dept., L.H.C.N. Labs., Univ. of Liège, 6 quai Banning, B4000 Liège, Belgium.

Note. Discussion open until August 1, 1992. To extend the closing date one month, a written request must be filed with the ASCE Manager of Journals. The manuscript for this paper was submitted for review and possible publication on February 23, 1991. This paper is part of the ***Journal of Structural Engineering***, Vol. 118, No. 4, April, 1992. ©ASCE, ISSN 0733-9445/92/0004-0926/$1.00 + $.15 per page. Paper

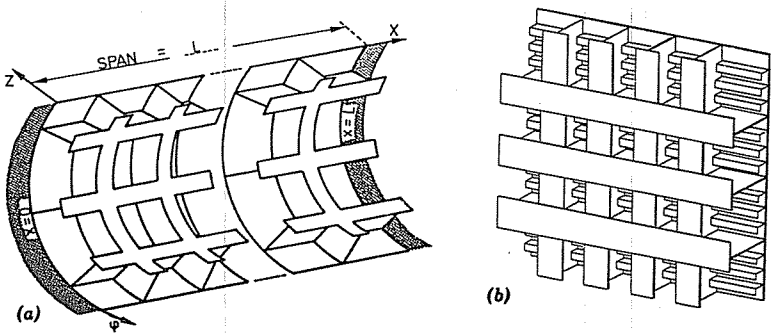

FIG. 1. Stiffened Cylindrical Shell (Rings and Stringers) and Orthotropic Plate with Crossbars

3 software, is a computation method dealing with cylindrical orthotropic shells (Rigo 1983a, b). As a result, LBR-3 gives displacements and stresses both with an equal level of accuracy, both being directly deduced and not one from the other. With this analytical method, results can be obtained at all points of the structure (sheathing, web, flange, web-flange junction, web sheathing junction).

For hydraulic structures, such as an orthotropic sheathing (Fig. 1), a navigation-dam gate, or a tidal surge barrier, frequent use is made of box girders, which are stiffened by longitudinal and transversal stiffeners. In these cases, the number of stiffeners and crossbars is so large that treating them by usual stress-analysis methods may become very expensive. For instance, the central processing unit (CPU) time for a simple sheathing lock gate (3,940 nodes and 21,000 degrees of freedom) is 90 min on an IBM 3081 (Aristaghes et al. 1986). By comparison, with LBR-3 for the aforementioned simple sheathing lock gate, it takes only 1 min on an IBM 4381.

The strongest advantage of this method is the discretization. Each stiffened shell or plate is considererd as one panel (Fig. 1); "panel" has the significance of an "element" in the finite-element method. However, a panel (shell or plate) includes all the stiffeners that are present; it is not necessary to split up the stiffener into smaller elements. For each panel of a structure, the analytical relationship of the solution (stresses and displacements) is obtained. It takes into account the compatibility conditions and the equilibrium equations that must be satisfied at the junction between two or more panels. Thus, it is, for instance, possible to study a stiffened square-box girder 100 m long, with only four of our elements (panels).

When the shells are cylindrical, which is the case of steel structures in the hydraulic field, the harmonic analysis methods are among the efficient ones (Bares and Massonnet 1966; Cheung 1976; Golberg and Leve 1957; Puckett and Gutkowski 1986; Schnobrich 1987). In these methods, loads and displacements, as well as stresses, are decomposed by Fourier series along a parallel direction to the cylinder-generating lines. The stiffened sheathing method is presented according to this principle.

Theoretical Statements

All the theoretical statements involved in the stiffened sheathing method (Rigo 1989a, b) cannot be included in this paper. Therefore, in presenting this method, only some of its originalities have been outlined.

R_x, R_φ = stringer and ring inertia moments with respect to middle surface of shell;
S_x, S_φ = coefficients considering stringer (ring) lateral bending stiffness;
T_x, T_φ = coefficients considering stringer (ring) torsional stiffness;
u = displacement along x-axis;
u', u^0 = derivative of u relative to x, derivative of u relative to φ;
v = displacement along φ axis;
v', v^0 = derivative of v relative to x, derivative of v relative to φ;
w = displacement along z-axis;
$w^{0\prime}$ = derivative of w relative to φ and x;
x, φ, z = axes of system;
X, Y, Z = specific pressures (N/m^2);
δ = thickness of shell;
ε_x, ε_φ = stringer and ring spacings;
λ = $n\pi/L$;
ν = Poisson coefficient;
φ_0 = shell degree of opening;
σ_x, σ_φ = stresses in shell along x- and φ-axes;
$\tau_{x\varphi}$ = shearing stress in $x\varphi$ plane (middle surface of shell);
Ω_x, Ω_φ = modified stringer (ring) transversal surface area, $\Omega_x = \omega_x E/d_x$; $\Omega_\varphi = \omega_\varphi E/d_\varphi$; and
ω_x, ω_φ = stringer (ring) transversal surface area.

The method is based on the analytical solution of the governing differential equations for orthotropic cylindrical shells with the shell thickness being held constant (Fig. 2). These differential equations (Dehousse 1961) result from the DKJ method (Donnell, von Kármán, and Jenkins). Many other methods are based on the same principle, but many of them have a very narrow application field and require many assumptions. Levy, Estanave, Timoshenko (1951), Vlassov (1962), Flügge (1960), and others deal with unstiffened plates and shells. Massonnet's method (Bares and Massonnet 1966), one of the first harmonic methods for stiffened structures, is specific to bridge decks. Using computers, Golberg and Leve (1957), and Gibson (1989) have also developed harmonic methods, but only for unstiffened plates. The finite difference method can also be used (Bushnell 1984, Jianping and Harik 1990). Some other very specific methods have been developed, such as Del Pozo's (1962) method, used to compute steel beams forming triangular links. A method that gives good results is the finite strip method (Cheung 1976), but it has been developed, above all, for unstiffened plates for bridge decks. Moreover, as for the usual finite element modeling schemes for commercial software (for which superelement techniques are often not available), the relative dimensions of each strip cannot be freely chosen. On the other hand, with an analytical method, the relative dimensions of the panels are not fixed; it is possible to put very small panels (10 cm width) beside large ones (10 m or 100 m width).

Many harmonic studies have been developed concerning the nonlinearity with the buckling aspect of the stiffened or unstiffened shells (Hutchinson and Amazigo 1967; Schnobrich 1987).

With LBR-3, nonlinear problems cannot be addressed, but, used together with FEM, these methods complement one another. For linear fields, designers could economically use the stiffened sheathing method (SSM) in order to design orthotropic steel structures composed of shells and plates. With this method, giving the displacements and the stresses around a small critical region of a structure (for instance, a hole in the sheathing or an unstiffened thin-skinned plate), the stress analysis in this region can be studied by FEM. Such a fruitful partnership might help in computing hydraulic steel structures for which design budgets are usually small and for which nonlinear problems are rare and always confined.

The LBR-3 application field is wide, including hydraulic steel structures (lock gate, movable weir, canal bridge, and tidal surge barrier), naval ar-

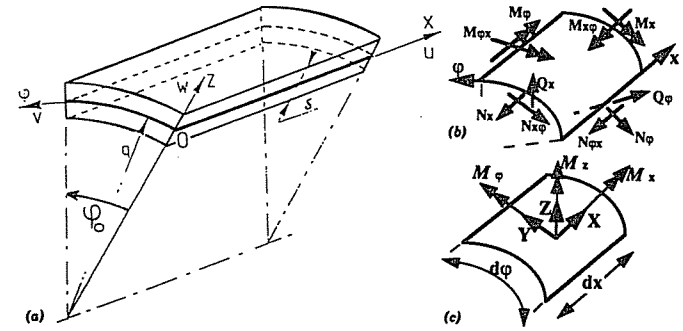

FIG. 2. Cylindrical Shell Element without Stiffening and Unitary Forces and Mo-

chitecture (tanker boat, barge, craft, oil tanker) (Rigo 1989a, b) and steel structure fields (shelving, formwork, floor, bridge deck).

Within the linear DKJ method (Dehousse 1961), no additional restrictions have been placed on the orthotropic shell with smeared-stiffener theory on the torsional stiffness, or on the lateral bending stiffness. The basic element is a cylindrical orthotropic shell where the length is L, q is the radius, δ is the thickness, and φ_0 is the shell degree of opening. The coordinate system is presented in Fig. 2, showing the x-axis being along the cylindrical generator, the φ-axis along the circumference, and the z-axis perpendicular to the shell. Displacements u, v, and w are associated with the x-, φ-, and z-axes. The reference shell is situated between the external and the internal surfaces (Fig. 2).

The stiffening includes three types of ribs (stringers, rings and crossbars) as shown in Fig. 1. These longitudinal and transversal ribs have, respectively, a spacing of ε_x and ε_φ. There are also the unitary forces (N_x, N_φ, $N_{x\varphi}$, $N_{\varphi x}$, Q_x, and Q_φ) and the unitary moments (M_x, M_φ, $M_{x\varphi}$, and $M_{\varphi x}$), which are calculated in relation to the middle surface (Fig. 2).

The middle surface (Fig. 2) receives the external loads which can be subdivided into X, Y, and Z, for specific pressures (N/m²), and $\bar{M}_x$, $\bar{M}_\varphi$, and $\bar{M}_z$, for the specific moments (N·m/m²). These loads enable one to apply dead load, hydrostatic pressure, pressures that can be varied along x- and φ-axes, as well as moments that are applied, for instance, at the extremities.

The six equilibrium equations containing the ten aforementioned variables can be determined

$$N'_x + \frac{N^0_{\varphi x}}{q} + X = 0 \quad \ldots\ldots (1)$$

$$\frac{N^0_\varphi}{q} + N'_{x\varphi} - \frac{Q_\varphi}{q} + Y = 0 \quad \ldots\ldots (2)$$

$$\frac{N_\varphi}{q} + \frac{Q^0_\varphi}{q} + Q'_x = Z \quad \ldots\ldots (3)$$

$$\frac{M^0_\varphi}{q} + M'_{x\varphi} - Q_\varphi + \bar{M}_x = 0 \quad \ldots\ldots (4)$$

$$M'_x + \frac{M^0_{\varphi x}}{q} - Q_x + \bar{M}_\varphi = 0 \quad \ldots\ldots (5)$$

$$N_{x\varphi} - N_{\varphi x} + \frac{M_{\varphi x}}{q} + \bar{M}_z = 0 \quad \ldots\ldots (6)$$

where f' = the derivative of f relative to x (df/dx) and f^0 = derivative of f relative to φ($df/d\varphi$).

At the moment, no hypothesis has been assumed. However, to solve the problem, it is necessary to introduce the following assumptions: the validity field of these developments is the elastic range of the DKJ simplications. These simplifications are the thin-shell assumptions (i.e., thickness << radius), the small deformations and the Love-Kirchhoff hypothesis. These hypotheses are sufficient to maintain a linear stress variation along the shell thickness.

In order to write the unitary expression of the forces and moments (Fig.

Jianping, P., and Harik, I. E. (1990). "Iterative FD solution to bending of axisymmetric conical shells." *J. Struct. Engrg.*, ASCE, 116(9), 2433–2445.

Puckett, J. A., and Gutkowski, R. M. (1986). "Compound strip method for analysis of plate systems." *J. Struct. Engrg.*, ASCE, 112(1), 121–138.

Rigo, P. (1989a). "Applications des développements harmoniques aux calculs des ouvrages hydrauliques métalliques," thesis presented to the Univ. of Liege, at Liege, Belgium, in partial fulfillment of the requirements for the degree of the Doctor of Philosophy (in French).

Rigo, P. (1989b). "Calculation of floating cylindrical structures." ATMA, 89ème Session, Paris.

Système d'analyse des milieux continus par eléments finis. (1988). Laboratoires des Techniques Aéronautiques et Spatiales, Samtech, Univ. of Liege, Liege, Belgium (in French).

Schnobrich, W. C. (1987). "Different methods of numerical analysis of shells." *IASS Bulletin No. 94.*

Scordelis, A. C., and Lo, K. S. (1964). "Computer analysis of cylindrical shells." *J. ACI*, 61(5).

Timoshenko, S. (1951). *Théorie des plaques et des coques.* Paris et Liège, Librairie Polytechnique Ch. Beranger (in French).

Vlassov, B. Z. (1962). *Pièces longues en voiles minces.* Eyrolles, Paris (in French).

Appendix II. Notations

The following symbols are used in this paper:

$\bar{A}, \bar{B}, \bar{C}, \ldots, \bar{K}$ = constants defined in (23);
a, b, c, d = parameters of end force functions $F(\varphi)$;
D = $E\cdot\delta/(1-\nu^2)$;
d_x, d_φ = maximal values of e_x stringer width and e_φ ring width;
d^* = length of end segments ($x = 0, x = L$) on which loads are applied;
E = modulus of elasticity;
e, f, g, h = parameters of end moments functions $G(\varphi)$;
e_x or $e_x(z)$, e_φ or $e_\varphi(z)$ = stringer and ring widths according to z-coordinate;
F or $F(\varphi)$ = analytical relationship of end forces;
$f(\varphi), f(x)$ = Heaviside functions;
$G(\varphi)$ = analytical relationship of end moments;
H_x, H_φ = stringer and ring static moments related to middle surface of shell;
K = $E\delta^3/12(1-\nu^2)$;
L = span of shell along x-axis;
L_x, L_φ = coefficients considering stringer (ring) lateral bending stiffness;
M_b = theoretical end moments;
$M_x, M_\varphi, M_{\varphi x}, M_{x\varphi}$ = unitary moments;
$\bar{M}_x, \bar{M}_\varphi, \bar{M}_z$ = specific moments (N·m/m²);
N_b = theoretical end forces;
$N_x, N_\varphi, N_{x\varphi}, N_{\varphi x}$ = unitary forces;
n = term number of Fourier series;
Q_x, Q_φ = unitary forces;

can be carried out within one day (mesh modeling data correction, computing—3 hr CPU on a Macintosh II, printing, and result analysis).

Conclusion

The Fourier series expansion for cylindrical shell analysis is a well-known method, but the stiffened sheathing method presents several improvements. It allows the computing of orthotropic cylindrical shells while considering the real position and geometry of each rib. The spacing and the dimensions could change; it is not a smeared-stiffener theory.

One other particularity of the method is that it is possible to compute structures that are composed of many stiffened shells and plates. Developments that establish an efficient computation tool, the LBR-3 software, have been presented. The main advantages and qualities of this software are: speed, simplicity and accuracy, and, of course, ease. LBR-3 enables one to compute very complex structures, such as curved stiffened sheathing, navigation-dam gate, tidal surge barrier, lock gate, canal bridge, etc. The stiffened sheathing method has been confirmed as an efficient alternative to other numerical techniques for analyzing structures composed by stiffened plates and cylindrical shells.

To increase the application field of the stiffened sheathing method, N_b end forces and M_b end moments that are applied at both ends of the shells, have been added to the classical external forces. Thus, it is now possible to compute many structures with many kinds of boundary conditions using the Fourier series.

Appendix I. References

Aristaghes, P., Lebreton, P., and Vansteenkiste, A. (1986). "Calcul des portes d'écluses maritimes" (in French). *Bulletin of the Perm. Int. Ass. of Nav. Congr.*, France, 52, 89–107.

Bares, R., and Massonnet, C. (1966). "Le calcul des grillages de poutres et dalles orthotropes" (in French). Dunod, Paris.

Bushnell, D. (1984). "Computerized analysis of shells-governing equations." *Comput. Struct.*, 18(3), 471–536.

Cheung, Y. K. (1976). *Finite strip method analysis in structural analysis.* Pergamon Press, Elmsford, N.Y.

Dehousse, N. M. (1961). "Les bordages raidis en construction hydraulique." *Mémoires du Centre d'Etudes, de Recherche et d'Essais Scientifiques du Génie Civil (Nouvelle Séries)* (in French), Vol. 1, Univ. of Liège, Belgium.

Dehousse, N. M. (1961). "Les bordages raidis en construction hydraulique" (in French). *Mémoires du Centre d'Etudes, de Recherche et d'Essais Scientifiques de Génie Civil (Nouvelle série),* Vol. 1, Univ. of Liège, Belgium.

Del Pozo, F. (1962). "Cubiertas laminares cilindricas formadas por una malla triangular de perfiles metalicos." No. 176, Consejo superior de investigaciones cientificas, Instituto tecnico de la construccion y del cemento, Madrid, Spain (in Spanish).

Flügge, W. (1960). *Statique et dynamique des coques* (in French). Eyrolles, Paris, France.

Fonder, G. A. (1985). *SAPLI 5—User guide.* Univ. of Liège, Belgium.

Gibson, J. E. (1989). "The development of general multi shell programs using a micro computer." *Numer. Methods,* IASS, Madrid, Spain.

Golberg, J. E., and Leve, H. L. (1957). "Theory of prismatic folded plate structures." *Mémoires AIPC,* Int. Assoc. for Bridge and Struct. Engrg., Zurich, Switzerland.

Hutchinson, J. W., and Amazigo, J. D. (1967). "Imperfection-sensitivity for ec-

two constants D and K, which are dependent on the material properties (modulus of elasticity E, Poisson ratio ν), the procedure is as follows.

The equilibrium of an infinitesimal element of two dimensions must be considered. The third dimension is not considered, since only the middle surface is being considered. In order to write the equilibrium of this element, unitary forces and moments calculated in relation to the middle surface have been introduced. For instance:

$$N_x = \int_{-\delta/2}^{+\delta/2} \sigma_x \left(1 + \frac{z}{q}\right) dz \quad \ldots\ldots (7)$$

$$M_x = -\int_{-\delta/2}^{+\delta/2} \sigma_x \left(1 + \frac{z}{q}\right) z\, dz \quad \ldots\ldots (8)$$

Taking into account the stress-deformation relationships

$$\sigma_x = \frac{E}{1-\nu^2}\left[u' + \nu\frac{v^0}{q} + \nu\frac{w}{q} - z\left(w'' + \nu\frac{w^{00}}{q^2}\right)\right] \quad \ldots\ldots (9)$$

$$\sigma_\varphi = \frac{E}{1-\nu^2}\left[\frac{v^0}{q} + \frac{w}{q} + \nu\,(u' - zw'') - z\frac{w^{00}}{q^2}\right] \quad \ldots\ldots (10)$$

$$\tau_{x\varphi} = G\left[\frac{u^0}{q} + v' - 2z\frac{w^{0\prime}}{q}\right] \quad \ldots\ldots (11)$$

Eqs. (12) and (13) for an unstiffened shell are obtained as

$$N_x = \frac{D}{q}(u'q + \nu v^0 + \nu w) \quad \ldots\ldots (12)$$

$$M_x = \frac{K}{q^2}(q^2 w'' + \nu w^{00}) \quad \ldots\ldots (13)$$

With stringers (Fig. 3), (7) and (8) are no longer valid and must be modified as follows:

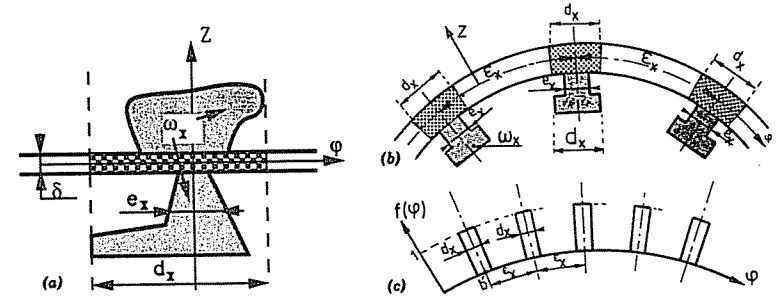

FIG. 3. Diagram of $f(\varphi)$ Functions, which Permit Consideration of Exact Location

$$N_x = \int_{-\delta/2}^{+\delta/2} \sigma_x \left(1 + \frac{z}{q}\right) dz + f(\varphi) \int_{\omega_x} \sigma_x \frac{e_x}{d_x} dz \quad \ldots\ldots\ldots\ldots\ldots\ldots (14)$$

$$M_x = -\left[\int_{-\delta/2}^{+\delta/2} \sigma_x \left(1 + \frac{z}{q}\right) z\, dz + f(\varphi) \int_{\omega_x} \sigma_x \frac{e_x}{d_x} z\, dz\right] \quad \ldots\ldots\ldots\ldots (15)$$

where e_x = the stringer width according to the z coordinate = $fct(z)$; d_x = the maximum value of the e_x stringer width; ω_x = the stringer transversal surface area; and $f(\varphi)$ = a function that is 1 under the stringer, and 0 elsewhere (see Fig. 3).

The $f(\varphi)$ functions [$f(x)$ for the rings] are composed of Heaviside ones, which enable one to obtain functions perfectly compatible with the structure geometry (Fig. 3). They are equal to unity and cancel out each other's spaces (d_x and d_φ) where the ribs act. These functions permit the consideration of the exact location of each stringer [or ring for an $f(x)$ function]. Hence, the geometric dimensions of two stringers (symmetric or eccentric) fixed on the same shell can be different. This is one of the most important particularities of this method. Many other methods use the smeared stiffener theory (Bares and Massonnet 1966; Hutchinson and Amazigo 1967).

After integration of (14) and (15), N_x and M_x become

$$N_x = \frac{D}{q}(u'q + \nu v^0 + \nu w) + f(\varphi)(u'\Omega_x - w''H_x) \quad \ldots\ldots\ldots\ldots\ldots (16)$$

$$M_x = \frac{K}{q^2}(q^2 w'' + \nu w^{00}) - f(\varphi)(u'H_x - w''R_x) \quad \ldots\ldots\ldots\ldots\ldots (17)$$

where Ω_x = the modified stringer transversal surface area ($\Omega_x = \omega_x \cdot E/d_x$); H_x = the static moment related to the middle surface; and R_x = the moment of inertia with respect to the middle surface.

Eqs. (16) and (17) show the precise position of each stringer is accurately considered. Indeed, $f(\varphi)$ equals zero between two stringers (Fig. 3); so, (12) and (13), which are valid for unstiffened shells, are again found to be valid.

The $N_{x\varphi}$ and $M_{x\varphi}$ relationships can also be obtained as

$$N_{x\varphi} = D\frac{1-\nu}{2}\left[v' + \frac{u^0}{q}\right] + f(\varphi)S_x\left[v' + \frac{u^0}{q}\right] \quad \ldots\ldots\ldots\ldots\ldots (18)$$

$$M_{x\varphi} = K(1-\nu)\frac{w^{0\prime}}{q} + f(\varphi)\left[T_x\frac{w^{0\prime}}{q} + L_x\left(v' + \frac{u^0}{q}\right)\right] \quad \ldots\ldots\ldots (19)$$

where S_x and L_x = two coefficients considering the lateral (tangent to the shell) bending stiffness; and T_x = a coefficient taking into account the torsional stiffness. These S_x and L_x coefficients must be carefully determined because they are very important for the transverse shear deformations (seen hereafter in the numerical verifications).

For the rings, N_φ, $N_{\varphi x}$, M_φ, and $M_{\varphi x}$ are to be obtained. The Q_x and Q_φ unitary forces are determined from the moment equations [(4) and (5)] by replacing the already-computed unitary forces and moments.

Next, by replacing the unitary forces and moments with their analytical expressions in (1), (2), and (3), a system of three differential equations with

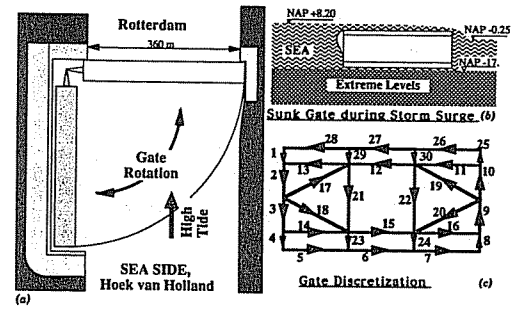

FIG. 9. Tidal Surge Barrier and Its Discretization with 30 Elements

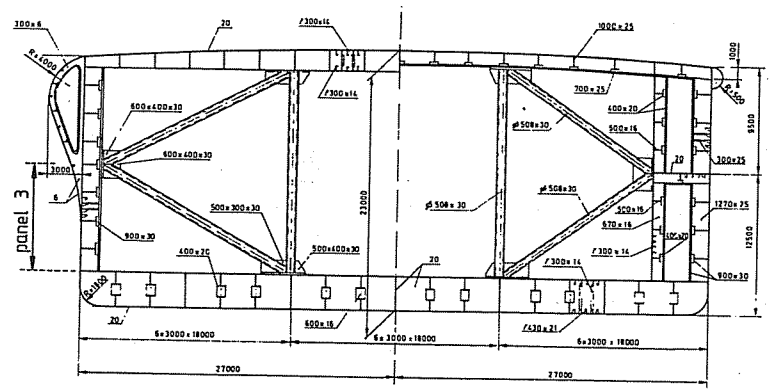

FIG. 10. Cross Section of Tidal Surge Barrier

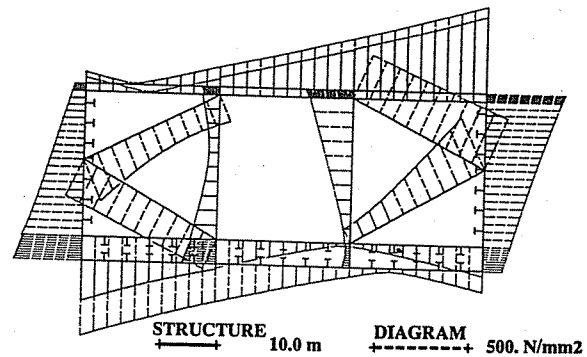

FIG. 11. von-Mises Comparison of Stresses at Midspan

in order to use LBR-3 software. Thus, it can be easily understood how attractive LBR-3 is to the designer.

As an example, Fig. 11 shows the diagram of the von-Mises comparison

to the other two, and, owing to the simplification of this discretization, SSM-1 will be regarded as the best one. For the discretization, SSM-1, the lateral bending stiffness contribution is absent ($S_x = L_x = 0$), but for the other two, this contribution still exists, although minute. So the difference between the SSM-1 and SSM-2 results comes from the fact that with the SSM-2 solution, the lateral bending stiffness of the flange is small but present. However, this small contribution is enough to produce the difference in the results.

Stiffened Plate with Participation of Flange in Lateral Bending Stiffness

If the stringer is fixed with gussets (Fig. 6), the contribution of the flange to the plate is important (S_x and L_x not nil). For the SSM-1 discretization, the results are given in Table 2 and are compared with the theoretical results of the beam and plate bending theory based on smeared-out rib properties. The comparison is excellent and shows how easy it is with LBR-3 to consider many gussets without the need to discretize them.

Application to Hydraulic Structure

The design and the computation of a tidal surge barrier will show, as succinctly as possible, that the LBR-3 software qualities are speed, accuracy, simplicity, and ease. This example is related to the construction of a tidal surge barrier to be built in the entrance channel of Rotterdam Harbor. The constraints include the requirement of maintaining an opening of at least 360 m to allow navigation to occur without hindrance.

The complexity of the structure does not allow presentation of all the relevant information here. For more details, see Dehousse and Rodriguez (1990).

In brief, the main features (Figs. 9 and 10) are: 390 m span (360 m + 2 × 15 m for the supports), 22 m height, 54 m width, and 55,000 metric tons weight. A main watertight box girder allows floating with a draught limited to 3 m. The extreme levels that must be considered and the discretization for computation are shown in Fig. 9. It needs 30 panels, 24 are stiffened (longitudinal and transverse stiffeners and crossbars), and the remaining six panels (17–22) represent the pillars. The importance of the stiffening of this structure demonstrates the advantages of LBR-3 software very well. For example, consider panel 3 (Figs. 9 and 10). Its main characteristics are: an overall dimension of 9.5 m × 390 m = 2,000 m², three crossbars with length of 390 m, 79 transversal stiffeners of length 7.9 m, and a total of 5,850 m of longitudinal stiffeners. All these elements require 11 data lines

TABLE 2. Deformation of Midspan (with Flange Contribution)

Method (1)	Displacement v (mm) along axis φ (2)	(3)	Displacement u (mm) along axis x (4)	(5)
LBR-3 (SSM-1) 1 panel, 6 stringers,[a] 8 equations	7.31	7 terms	2.11	7 terms
	7.70	1 term	2.05	1 term
Bending Theory[b]	7.10		2.25	

[a]Stringer modeling is made within modeled stiffened panel.
[b]Smeared stringers.

expressing the stiffened cylindrical shell, are functions of only the u, v, and w displacements and their spatial derivatives.

$$D(qu'' + vv^{0\prime} + vw') + \frac{D}{q^2}\frac{(1-\nu)}{2}(u^{00} + qv^{0\prime}) + f(x)\left[\frac{S_\varphi}{q}\left(v^{0\prime} + \frac{u^{00}}{q}\right)\right] + \frac{f^0(\varphi)}{q}\left[S_x\left(v' + \frac{u^0}{q}\right)\right] + f(\varphi)\left[\Omega_x u'' - H_x w''' + \frac{S_x}{q}\left(v^{0\prime} + \frac{u^{00}}{q}\right)\right] + X = 0 \quad \ldots\ldots\ldots\ldots (20)$$

$$\frac{D}{q^2}(v^{00} + w^0 + vqu^{0\prime}) + \frac{D}{q}\frac{(1-\nu)}{2}(u^{0\prime} + qv'') + f(x)\left[\frac{\Omega_\varphi}{q^2}(v^{00} + w^0) - \frac{H_\varphi}{q^3}w^{000} + S_\varphi\left(v'' + \frac{u^{0\prime}}{q}\right)\right] + \frac{f'(x)}{q}\left[S_\varphi\left(v' + \frac{u^0}{q}\right)\right] + f(\varphi)\left[S_x\left(v'' + \frac{u^{0\prime}}{q}\right)\right] + Y = 0 \quad \ldots\ldots (21)$$

$$\frac{D}{q^2}(v^0 + w + vqu') + \frac{K}{q^4}w^{0000} + \frac{2K}{q^2}w^{00\prime\prime} + Kw'''' + f(x)\cdot\left[\frac{\Omega_\varphi}{q^2}(v^0 + w) - \frac{2H_\varphi}{q^3}w^{00} - \frac{H_\varphi}{q^3}v^{000} + \frac{R_\varphi}{q^4}w^{0000} + \frac{T_\varphi}{q^2}w^{00\prime\prime} + \frac{L_\varphi}{q}(v^{0\prime\prime} + u^{00\prime})\right] + f(\varphi)\left[\frac{T_x}{q^2}w^{00\prime\prime} + \frac{L_x}{q}\left(v^{0\prime\prime} + \frac{u^{00\prime}}{q}\right) - H_x u''' + R_x w''''\right] + \frac{f^0(\varphi)}{q}\left[\frac{T_x}{q}w^{0\prime\prime} + \frac{L_x}{q}\left(v'' + \frac{u^{0\prime}}{q}\right)\right] + f'(x)\left[\frac{T_\varphi}{q}w^{0\prime\prime} + \frac{L_\varphi}{q}\left(v'' + \frac{u^{0\prime}}{q}\right)\right] = -\frac{\bar{M}_x^0}{q} + M_\varphi' + Z \quad \ldots\ldots\ldots (22)$$

where Ω_x, H_x, T_x, L_x, S_x, and R_x = parameters depending on the stringer geometry, and Ω_φ, H_φ, T_φ, L_φ, S_φ, and R_φ = parameters depending on the ring geometry. The $f^0(\varphi) = df(\varphi)/d\varphi$ and $f'(x) = df(x)/dx$ functions are derivatives of the Heaviside ones. Thus, these are Dirac functions, which are always zero except under the ribs where their integrals equal unity.

The principle of solving this system [(20), (21), and (22)] is based on the transformation of the three differential equations by a classical system of three equations and three unknowns. The coefficients are the differential operators, and the unknowns are the u, v, and w displacements. After calculation, only one eighth-order differential equation of w with two variables (x and φ) is obtained [(23)]:

$$\bar{A}\cdot w^{''''} + \bar{B}\cdot w^{''''} + \bar{C}\cdot w^{''''''} + \bar{D}\cdot w^{''''} + \bar{E}\cdot w^{''''} + \bar{F}\cdot w^{''''} + \bar{G}\cdot w^{''''} + \bar{I}\cdot w^{''''} + \bar{J}\cdot w^{''''} + \bar{K}\cdot w^{''''} = 0 \quad \ldots\ldots (23)$$

where $\bar{A}, \bar{B}, \bar{C}, \ldots, \bar{K}$ coefficients = constants that depend only on the geometric characteristics of the shell and its stiffeners. They depend also on the mechanical properties of the material (E, ν).

To obtain an equation with two independent variables, the displacements are developed using Fourier series expansion:

$$w(x, \varphi) = \sum_{n=1}^{\infty} w(\varphi)\sin\frac{n\pi x}{L} \quad \ldots\ldots (24)$$

$$v(x, \varphi) = \sum_{n=1}^{\infty} v(\varphi)\sin\frac{n\pi x}{L} \quad \ldots\ldots (25)$$

$$u(x, \varphi) = \sum_{n=1}^{\infty} u(\varphi)\cos\frac{n\pi x}{L} \quad \ldots\ldots (26)$$

There is no right-hand side in (23) because only the load lines are considered. They are applied on a $q\cdot d\varphi$ infinitesimal space across a line along the x-axis. The analytical relationship of w is obtained after integration of the general solution [(23)] along the φ-axis for the real load distribution (Dehousse 1961).

The real actions of the stringers on the shell are determined by the solution of a system of integral equations that are well known as the Volterra-Fredholm equations of the second kind. The kernels of these integral equations come from the introduction of the Green functions in the analytical relationships of the three unitary force lines and the two unitary moment lines. So, the stiffened shell can be computed as an unstiffened shell where, not only do the external loads act, but also five load lines at each stringer (or ring) position act.

After solving the integral equations for the displacements, the first results are the analytical relationships of the u, v, w displacements according to the x-, φ-, and z-coordinates. By replacing these in (9), (10), and (11), the analytical expressions for the stresses may be obtained. For $z = 0$, stresses are determined in the middle surface of the shell. Knowing the x, φ, and z stiffener coordinates, the stresses at every point of a stiffener can also be computed (for instance: in the web, in the flange, etc.). The analytical expressions that result from the aforementioned principles will not be developed here. These computations are too long and not useful to the reader. For more details, refer to the main work of the author (Rigo 1989).

Structures with Particular End Conditions

The sine-series decomposition of $w(x, \varphi)$ [(24)] implies that the other displacement expressions are $v(x, \varphi)$ as $\sin \lambda x$ [(25)], and $u(x, \varphi)$ as $\cos \lambda x$ [(26)]. So, at the boundaries ($x = 0$ and $x = L$), the w and v displacements vanish, but the u longitudinal displacement and the $w' = dw/dx$ rotation do not. Hence, theoretically, the $x = 0$ and $x = L$ extremities must always be simply supported; the two other zones ($\varphi = 0$ and $\varphi = \varphi_0$) can be free, fixed, simply supported, or common with other panels.

As far as the hydraulic structures are concerned, many box girders and

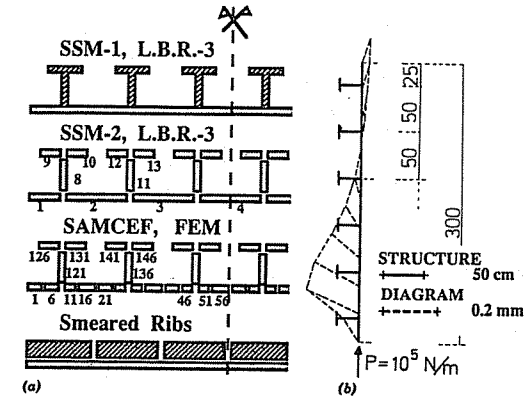

FIG. 8. Used Discretizations (FEM, LBR-3, and Bending Theory) and for SSM-1 Discretization, v and w Displacements at Midspan

TABLE 1. Deformation at Midspan (without Flange Contribution)

Method (1)	Displacement v (mm) along axis φ (2)	Displacement u (mm) along axis x (3)
SAMCEF, FEM[c] 210 elements, 2,854 equations	18.10	5.14
LBR-3 discretization SSM-1,[a] 7 terms, 1 panel, 6 stringers, 8 equations	20.17	5.81
LBR-3 discretization SSM-2,[b] 7 terms, 25 panels, 200 equations	19.50	5.57

[a]The stringer modeling is made within the modeled stiffened panel.
[b]Stringers modeled with unstiffened plate panels.
[c]Stringers modeled with unstiffened plate elements.

mations will be different (warping). Such behavior cannot be studied with the present method except by using a secondary discretization, the so-called SSM-2. This second discretization needs more elements and is also more expensive. There are seven unstiffened panels to discretize the skin plate and three for each stringer, which are, therefore, modeled by unstiffened panels as for the FEM modeling. Thus, there are 25 panels ($7 + 3 \times 6 = 25$) and then a system of 200 (25×8) equations to solve. Such a discretization could also be used by the finite strip method.

The SSM-2 discretization allows stringers to work separately of the skin plate because, in this case, the assumption that sections remain straight during the bending is no longer a restriction. The representation of the transmission of loads between stringers and sheathing corresponds to reality. On the other hand, for the SSM-1 discretization, the theoretical assumption that sections remain straight during the bending is verified.

The v and u displacements for the three discretizations (FEM, SSM-1, and SSM-2) are presented in Table 1. There is good correlation between the FEM and the SSM-2 solutions. The SSM-1 results (Fig. 8) are very close

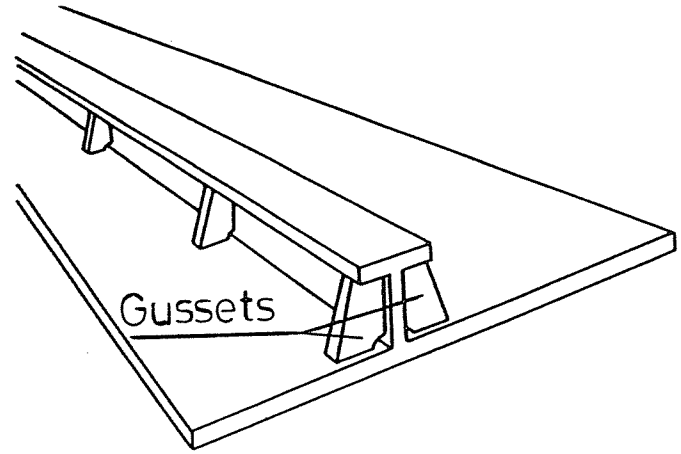

FIG. 6. Stringer Fixed on Skin Plate with Gussets

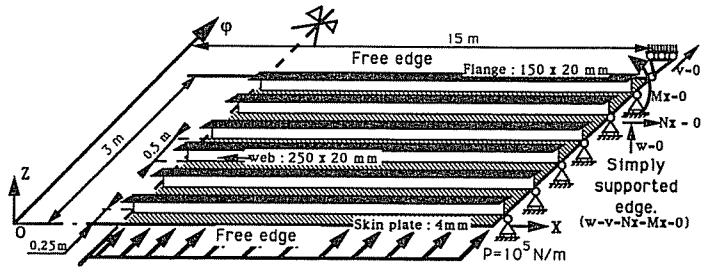

FIG. 7. Stiffened Plate Loaded in Its Plane

Stiffened Plate without Participation of Flange in Lateral Bending Stiffness

This is the case where there are no gussets between the flanges and the skin plate. Thus, the transverse shear deformation will be of great significance because the load will mainly be supported by the sheathing alone. Having no gussets, the forces cannot be transmitted from the skin plate to the flanges as the webs are not strong enough.

The study of this stiffened plate has been done by FEM to confirm the LBR-3 results. Taking into account the symmetry, the finite element discretization is the following (Fig. 8): 24 rows of five plate elements for the skin plate and three rows of five plate elements per stringer (one row per web and two rows per flange). There is a total of 210 unstiffened plate elements with 32 degrees of freedom for each, so with the fixed nodes, 2,854 unknowns had to be calculated.

Using the stiffened sheathing method (SSM), the results with two discretizations are presented (Fig. 8). The first one, the so-called SSM-1, is related to a discretization having only one stiffened panel including the six stringers without participation of the flange in the lateral bending stiffness [$S_x = L_x = 0$, see (18) and (19)]. These stringers are modeled as shown in Fig. 3.

stiffened sheathings are simply supported. Nevertheless, many also have other boundary conditions. For instance, box girders of radial gates are elastically supported by both of their arms (at the box-girder ends, u and w' are not free), and some orthotropic steel decks must be computed as fixed (at the ends, $u = w' = 0$).

Desiring to extend the field application of the stiffened sheathing method, investigations (Rigo 1989a, b) have shown that end forces (N_b) and moments (M_b) can be applied to the $x = 0$ and $x = L$ ends to simulate particular boundary conditions (elastically or rigidly supported). These N_b forces and M_b moments do not allow for the simulation of free ends ($w = v = 0$ at $x = 0$ and $x = L$) because the aforementioned conditions can never be transgressed [see (24) and (25)].

Later, a general overview of our present investigation will show that such N_b forces and M_b moments are consistent with harmonic analysis of the stiffened shell.

Among the X, Y, and Z external forces (Fig. 2), end forces N_b and end moments M_b are included and are applied at both ends of the plates and the shells of the structures (Fig. 4). These end forces and end moments permit the simulation, for example, of axial force as well as bending and torsion moments that the supporting arms of a radial gate transmit to the main box girder.

As far as the end forces N_b are concerned, the development of two asymmetrical end loads F are used, and so the analytical solution of a shell submitted to two asymmetrical longitudinal loads F applied at both ends is obtained. The analytical expression of the N_b end forces is:

$$N_b(x) = \sum_{n=1}^{\infty} \left[\frac{4}{(2n-1)\pi d^*} F(-1)^{n+1} \cdot \cos \frac{(2n-1)\pi(L-2d^*)}{L} \sin \frac{(2n-1)\pi x}{L} \right] \quad \ldots\ldots\ldots\ldots\ldots\ldots (27)$$

where $F = F(\varphi)$ = the applied force at unit length along $o\varphi$; F = a function of φ [(28)], and d^* = the length of end segments where the F force is applied.

For the end moments, the same methods is used. However, there is an important difference as only the derivative of the external load M_φ is present

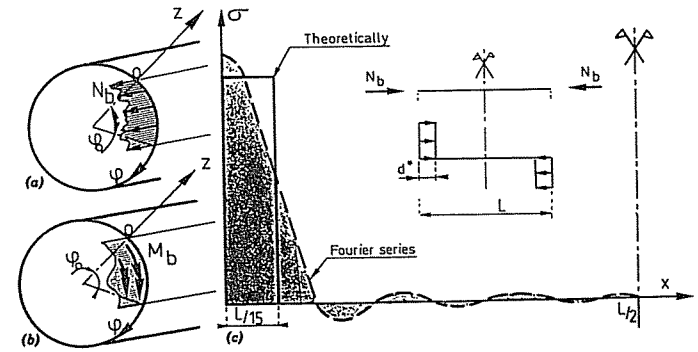

FIG. 4. Development of Asymmetrical N_b End Forces ($d^* = L/15$). N_b End Forces

in the differential equations [(20), (21), and (22)]. So $dM_b(x)/dx$, the derivative of the M_b end moments, must be considered.

Fourier Series Expansion of End Forces and Moments

If an exact load decomposition must be obtained, the development of the end moments requires a very large number of terms (50–100 terms). In practice, concentrated loads do not exist. They are always more or less applied on d^* length segments. So, N_b end forces and M_b end moments are always applied on such d^* segments near the ends. Satisfactory results with only the first seven terms of the Fourier series are obtained with an acceptable accuracy. For $d^* = L/15$, Fig. 4 shows the theoretical end force (solid line) and the practical one (dotted line), which has been applied by using the Fourier series expansion.

The d^* length is one of the most important parameters to determine the accuracy of the results. However, in practice, this is influenced by the structure geometry and some other practical considerations. For instance, the junction between the box girder of a radial gate and the arms must be very strong, so there is a minimum (practical) width for arms and there are also many strengthening pieces (plates, gussets, etc.). Therefore, the results in the end regions will always be approximate. After many trials, it has been seen that the most economical solution is to take d^* in the range of $L/15$ (L = span), which assures an acceptable level of accuracy.

Computation of Elastically Supported Structures

Using the N_b end forces and M_b end moments, computation of elastically supported structures becomes possible.

Because of (24), (25), and (26), the end sections are like partition walls that are rigid in their respective planes ($w = v = 0$). The perpendicular displacement to each plane is free, which is the case of the longitudinal displacements u. In spite of these conditions, it is possible to take into account the particular boundary conditions (fixed, elastically supported). Consider a radial gate loaded by hydraulic pressure (hydrostatic and hydrodynamic pressures). The box girder and the supporting arms behave as portals (Fig. 5).

The end sections of the gate cannot have any deformation as would a simply supported gate. If the end of a supporting arm is subjected to a general rotation ϕ (Fig. 5), the u longitudinal displacements and the dw/dx rotations at the junction box girder/arm are readily known according to the

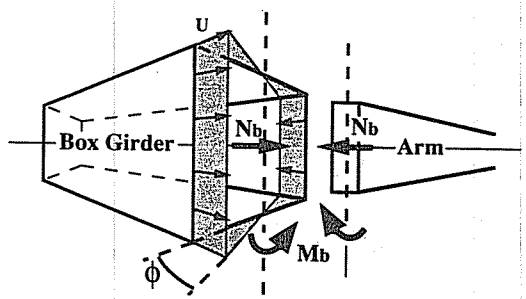

FIG. 5. Plan of Portal, Box Girder and One Supporting Arm of Radial Gate. End Deformation of Box Girder

ϕ variable. Therefore, it is necessary to apply both N_b end forces and M_b end moments at the extremities, and both must have compatibility between the end displacements of the box girder and the displacements resulting from the arm rotation.

At the box girder/arm junction, it is necessary to check the compatibility of the u displacements and the dw/dx rotations. The mechanism of the portal is then split up in two parts—the arm is one and the box girder is the order—and these two are analyzed separately.

Determining End Effects

The method used to determine the end forces and moments when the u displacements and the dw/dx rotations are fully known is the following.

The N_b and M_b theoretical relationships present important inconveniences because the subsequent analytical developments would be cumbersome to handle (Rigo 1989a, b). For simplicity and rationalization purposes, the third-degree polynomial development has been chosen for the functions representing the end effects. Let $F(\varphi)$ and $G(\varphi)$ [(28) and (29)] be the end forces and moments functions where a, b, c, d and e, f, g, h are, respectively, unknown parameters of the end force function and the end moment function.

$$F(\varphi) = a(q\varphi^3) + b(q\varphi)^2 + c(q\varphi) + d \quad \ldots\ldots\ldots\ldots\ldots\ldots\ldots\ldots (28)$$

$$G(\varphi) = e(q\varphi)^3 + f(q\varphi)^2 + g(q\varphi) + h \quad \ldots\ldots\ldots\ldots\ldots\ldots\ldots\ldots (29)$$

Each parameter is in fact, the multiplicate coefficient of a unitary end force or moment. Practically, the coefficients $a, b, c, d, \ldots, h$ are obtained by imposing, point by point, the condition of displacement continuity and rotation continuity between the box girder and the supporting arms. Assume a structure composed of n shells in which there are $8 \cdot n$ unknown parameters that are determined by imposing $8 \cdot n$ continuity conditions at some structural points.

Examples of Numerical Verifications of Stiffened Sheathings Method

There are several generally accepted verifications related to unstiffened shells (Rigo 1989a, b). For these verifications, the LBR-3 results were compared with FEM software such as SAMSEF (1988), SAPLI (Fonder 1985), and other methods (Scordelis and Lo 1964; Vlassov 1962).

We hereby present verifications of orthotropic plates. Their aim is to evaluate the flange contribution to the lateral (tangent to the shell) bending stiffness of the stringers. This contribution is very important because the transverse shear deformations are of great significance in the case of stiffened plates. It is interesting to see how much the flanges help the skin plate (sheathing) when they are fixed by gussets (Fig. 6) or without gussets.

A plate, 15 m wide and 3 m high, loaded in its plane has been studied (Fig. 7). The load ($P = 1 \times 10^5$ N/m) was applied along the $x = 0$ coordinate line. The six stringer dimensions being very important (flange: 150 × 20 mm, web: 250 × 20 mm, and spacing: 0.5 m) in comparison to the skin-plate thickness ($\delta = 4$ mm), this example will better show the flange influence. The $x = 0$ and $x = 15$ m edges are simply supported ($w = v = N_x = M_x = 0$), and the two other ones ($\varphi = 0$ and $\varphi_0 = 3$ m) are free. Two